Vol. 04, Iss. 1 (2026) 95-112, DOI: 10.61552/JME.2026.01.010

Journal of Materials and Engineering

www.jme.aspur.rs

Review article

From Viscosity to Dielectric Breakdown: A Review of Rheoelectricity and Its Tribological Impact

Ahmadreza Aminian[a,*]

[a]*Islamic Azad University, Semnan, Iran.*

Keywords:

Rheoelectricity
Lubricant
Rheology
Tribology
Electric

* Corresponding author:

Ahmadreza Aminain
E-mail: araminian78@gmail.com

Received: 3 November 2025
Revised: 12 December 2025
Accepted: 12 January 2026

ABSTRACT

The electrical and magnetic properties of lubricants, along with their rheological properties, have always played an undeniable role in predicting the failure mechanisms of electromechanical equipment such as EVs. This article attempted to classify lubricants based on their performance with a criterion such as shear stability and resulting rheological models with two assumptions of the shear stress dependence/independence to shear rate, defining different lubricants rheological properties, and expressing their interaction outcome along with influence degree of environmental components such as local and instantaneous temperature and pressure using mathematical relations. Then, while defining rheoelectricity and affecting parameters, the lubricant's rheo-electrical properties and the way each is related to the lubricant's rheology under the effect of an electric field on lubricant film were investigated, resulted in an expression of each parameter effect on the lubricant rheo-electrical behavior with a cumulative index such as the Mason number. This article emphasizes the importance of rheoelectricity and the effect of rheo-electric properties on lubricants electromagnetic behavior under influence of both electric and magnetic fields. An attempt has been made to express Influenceability of lubricant rheology from electric fields and to provide an introduction to the electromagnetic behavior of lubricants.

1. INTRODUCTION

The increasing integration of electrical and electromechanical systems has led to a growing scientific interest in understanding how electromagnetic fields influence the behavior and reliability of lubricated contacts. Electrically induced surface damage, including frosting, fluting, and micro-pitting, has been documented in rotating machinery, electric motors, rolling bearings, and high-speed drives. These failures highlight the need for a deeper understanding of the interaction between the electrical properties of lubricants and their rheological response under operational conditions.

Despite extensive research on lubrication theory and tribological mechanisms, a unified framework describing the coupling between rheology and electrical behavior remains insufficiently developed. Classical lubrication models typically treat electrical effects as secondary phenomena, while electro-technical studies often overlook the influence of flow, shear, and viscosity on charge transport and dielectric behavior. This disconnect has prevented a comprehensive explanation of several electro-tribological degradation mechanisms.

To address this gap, the present review introduces and formalizes the concept of rheoelectricity, which characterizes the interplay between a lubricant's rheological properties and its electrical response. The aim is to provide clarity on the physical parameters that govern field-dependent lubricant behavior, enabling a more predictive understanding of electro-mechanically driven failure modes.

Since ancient times, industrial lubricants have always played a decisive role in heat dissipation and lubrication of surfaces involved in the stress exchange chain of various electromechanical equipment and therefore, their rheological properties have been continuously studied in order to provide a stable range of performance characteristics under influence of various factors, including heat, speed, environmental pollutants such as dust, water, and solvents. Lubrication between machine components, at least in order to reduce friction and prolonging life of their components, has been prevalent as long as human civilization, and there are signs that prove the application of lubrication knowledge in ancient times over past 4,500 years. Until the last two centuries, the lubricant selection was based solely on the proven experience since years ago leading to lessons learned about ability and performance of a typical lubricant's usage in a particular application. Accordingly, lubricant selection was made mainly with regard to its density while other rheological properties were not given much attention. This attention to density was such that until a century ago the only conceivable application for a viscometer was as a tool for comparing known and reliable vegetable or animal oils with unknown, new-coming mineral oils [1].

However, this rule was broken in 1886 with the introduction of the olive-oil thermo-viscosity equation by Osborne Reynolds, which intended to correlate dynamic viscosity with absolute temperature in degrees Kelvin in the form of an exponential function [2]:

$$\eta = ae^{-bT} \tag{1}$$

In Eq. (1), known as the Reynolds equation, η is the dynamic viscosity [cP], T is the oil's absolute temperature [K], and a and b are constants that can be calculated exclusively [2]. Although before Reynolds, others such as Hooke in 1684, Newton in 1686, Du Buat in 1786 [1], and Poiseuille in 1840 had attempted to express the importance of fluid viscosity and provide a mathematical definition for its heat sensitivity, it can be safely stated that prior to Reynolds, the role of lubricant viscosity in lubrication quality—especially in mechanical devices—was not properly understood [2].

In tribology, it is not possible to describe the interaction of each component present in a contact zone between two mechanical parts under lubrication without defining rheology and its related properties [1]. However, rheology is not limited to fluids and also applies to solids [3], with differences arising only from environmental conditions and material nature. The term rheology, first used in 1920 by Eugene Cook Bingham [4], is derived from the Greek word rheo, meaning "to flow" [3], and the suffix -logy. It refers to the study of the relationship between shear stress and strain in solids or between shear stress and shear strain rate in fluids [1].

In other words, rheology is dedicated to the study of how a material, essentially a liquid, flows and the mechanisms that govern it; However, soft materials, plastics, and other paste-like solids, if they flow rather than deform elastically under stress, are also subject to rheological study [4].

In a liquid fluid such as oil, shear stress is defined as [3]:

$$\tau = \frac{F}{A} \tag{2}$$

In Eq. (2), τ is the shear stress [Pa or N/m^2], F represents the shear force [N], and A is the shear cross-sectional area [m^2]. Applying a shear force to area A generates a velocity v in different layers of the oil film with a minimum film thickness h_{min} (Fig. 1).

Obviously, velocity is not the same everywhere throughout the h_{min}, which causes a difference in the shear rate in each layer of the oil film. This is where the shear rate γ shows its application among the shear difference between oil film different layers which can be defined as follows [3,5]:

$$\gamma = \frac{\mathrm{v}}{\mathrm{h_{min}}} \tag{3}$$

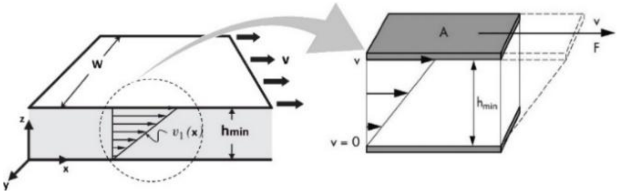

Fig. 1. Schematic representation of shear force–induced velocity distribution across the minimum oil film thickness $h_{\min}$, adapted from [3,5].

In Eq. (3), v is the velocity [m/s] and $\mathrm{h_{min}}$ is the minimum oil film thickness in [m]. Thus, the unit of measurement for the shear rate (or referred in some literature as strain rate, deformation rate, shear gradient, and velocity gradient [3]) γ can be expressed as [1/s or s^{-1}]. In mineral oils and lubricating greases for motor applications, the shear rate is in the range of 10^{-1} [6] ~10^{7} [3,6].

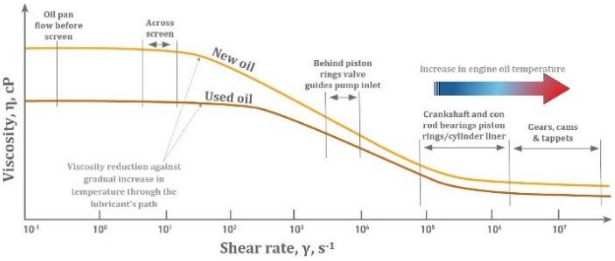

Fig. 2. Viscosity in terms of increasing shear rate in different section of engine lubrication [6].

Engine-oil viscosity, one of the most prominent applications of mineral lubricants, is strongly affected by shear rate in addition to temperature [2]. This behavior leads to the concept of shear stability, which describes an oil's resistance to mechanically induced viscosity loss. Based on this characteristic, lubricants are commonly classified into Newtonian fluids [3], shear-thinning non-Newtonian fluids, and shear-thickening (dilatant) fluids [6]:

- Oils with constant shear behavior, which are referred as Newtonian fluids [3], and single-grade engine oils such as SAE 40 are among the most prominent examples of such oils. The viscosity of this group of oils is not affected by shear rate (Figure 3).

Thus, in a Newtonian fluid, viscosity is not a function of shear rate and remains a function of temperature and pressure. In such a model of rheological behavior, if a fluid is placed between two parallel plates, one of which is sliding with respect to the other at a speed v (as Figure 1), the shear stress τ created in this fluid will increase linearly with the speed v; of course, this rule is valid for small speeds v and as the sliding speed v increases to a certain value, the shear stress τ reaches the limit of Newtonian behavior and its growth rate will gradually decrease. In fact, the limit of an oil's Newtonian behavior can be defined as a range of speeds determined by the oil's ultimate shear strength beyond which no increase in shear stress will be possible [1].

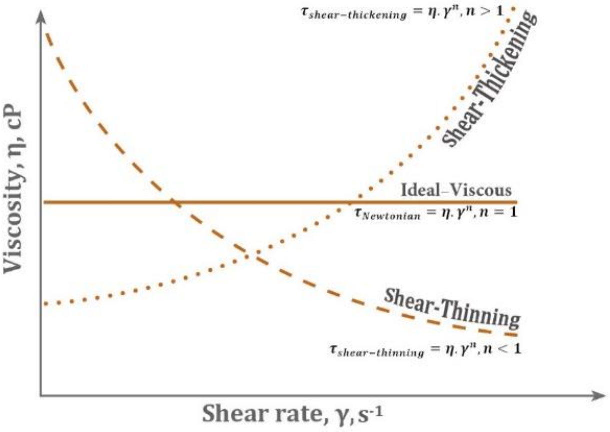

Fig. 3. Rheological behavior vs. shear stability, adapted from [3,6].

- Oils with shear thinning behavior that are non-Newtonian in nature (quasi-plastic) and lose their viscosity when mechanical stress is applied. All-year motor oils such as SAE 5W30 fall into this category.

- Oils with shear thickening behavior that are non-Newtonian in nature (dilatant) which their viscosity is strengthened and they regain their density when mechanical stress is applied under isothermal conditions [6].

The purpose of rheology is to define the relationship between stress and strain rate in fluid flow, whether or not Newton's law applies, in order to explain mechanical behavior [7]. Many industrial fluids exhibit non-Newtonian behavior [7], and even Newtonian fluids such as oils may display non-Newtonian or quasi-solid behavior under specific thermodynamic conditions [8]. Lubricating greases, for example, behave as viscoelastic-plastic solids [9,10], exhibiting more complex rheological behavior than Newtonian fluids.

Given these interpretations, the term rheological properties are often used broadly in the literature without detailed specification. In this paper, however, since the objective is to define rheoelectricity and rheo-electric properties of industrial lubricants, it is first necessary to clearly define rheological properties and rheological models, along with their respective influence on lubricant performance.

1.1 Definition and Scope of Rheoelectricity

Rheoelectricity is defined as the coupled interaction between a lubricant's rheological behavior and its electrical properties under mechanical, thermal, and electromagnetic loading. It describes how deformation-dependent parameters such as viscosity, shear-stress response, and flow regime correlate with field-dependent electrical characteristics, including conductivity, resistivity, dielectric constant, dielectric loss factor, capacitance, and dielectric breakdown strength. This coupling is essential for interpreting electrically induced degradation phenomena in tribological systems.

1.2 Scope and Nature of This Review

This article is structured as a scholarly literature review synthesizing the physico-mechanical properties and key parameters governing the tribological performance of lubricants under electric or magnetic fields. It evaluates published findings—including those of the present author and other researchers—to provide an integrated perspective on the current state of knowledge relevant to rheo-electric behavior.

2. RHEOLOGICAL MODELS

This section provides a detailed overview of the physical properties relevant to lubricant behavior under coupled mechanical and electromagnetic loading, including viscosity, shear behavior, pressure–viscosity response, and basic dielectric properties. Experimental studies have shown that dielectric permittivity of mineral and PAG oils exhibits strong pressure- and temperature-dependence in hydrodynamic bearing applications, reinforcing the coupling between rheological state and electrical response [11]. Accurate characterization of rheological and dielectric parameters relies on appropriate measurement methodologies, whose limitations and uncertainties must be considered when interpreting experimental lubricant data [12].

The Newtonian model for fluid behavior in lightly loaded bearings provides suitable explanation for rheological behavior of lubricating oils by describing how shear stress develops as a function of shear strain. Obviously, at low shear stresses and speeds the bearing temperature will also remain low. However, when these two parameters increased, the bearing operating temperature also goes up and, naturally, the viscosity of the lubricant cannot be assumed to be constant [1]. On the other hand, in EHL lubrication, the local oil pressure reaches 1 GPa [1,13] or in bearings where the oil pressure can reach 4 GPa or in automotive gearboxes where the oil film has a pressure of 2 GPa between the gears [13]; at such a pressure, the oil leaves its natural liquid state and exhibits a quasi-solid behavior [13]. Under such pressurized conditions, assuming static situation, the viscosity of the oil will reach several times its normal state [1,13]. For example, in the case of metal forming oils, this amount reaches 10 times [13]. With this in mind, the shear rate loses its proportionality to the shear stress [1] and hence Newton's law is no longer sufficient to describe the lubricant behavior.

For a long time, it was accepted that lubricating oils could exhibit non-Newtonian behavior under certain conditions of temperature and pressure; however, the first experimental measurement of the yield stress in oils under very high pressures occurred in 1941 [1]. The term "yield point", previously mentioned by Theodore Schwedoff in 1880 under the other name "stiffness-at-rest", is by definition the point where a fluid resists over the application of an external force to cause it to flow. Thus, the yield stress of a fluid is directly related to the dominance of the external forces acting on it over the internal forces of that fluid mass [3]. In order to predict the oil film formation and the action of tensile forces mechanism acting on it at heavy contact points, it is necessary to have access to a mathematical model describing behavior of the lubricant. In this regard, Newton in 1686 attempted to establish a linear relationship between shear rate and shear stress of a fluid, which led to Newton's model; However, oil under high pressures violates this rule and even small shear rates under high pressures will lead to very high shear stresses [1]. Such an error makes it impossible to use the Newtonian model at high pressures. After Newton, different models were proposed to describe the lubricant behavior under high pressures, which can be divided into two general categories according to the theoretical logic supporting each model.

2.1 Models with shear stress as a function of shear rate

This class of models, which mentioned in Table 1, originates from Newtonian models in which viscosity and shear stress as a function of temperature and pressure (but independent of time) [1].

Table 1. Rheological models assuming shear stress as a function of shear rate.

Model	Description	Comments
Schwedoff-Bingham	$\tau = \tau_0 + \eta\gamma$	Schwedoff [3], then Bingham [3,14-21]
Herschel-Bulkley	$\tau = \tau_0 + m\gamma^n$ $\begin{cases} n < 1 \longrightarrow \text{Shear} - \text{thinning} \\ n = 1 \longrightarrow \text{Schwedoff} - \text{Bingham} \\ n > 1 \longrightarrow \text{Shear} - \text{thickening} \end{cases}$	Herschel & Bulkley [22-23], to expand the S-B scope [21].
Casson	$\tau^{p^{-1}} = \tau_0^{p^{-1}} + (\eta\gamma)^{p^{-1}}$	Aimed for printing in textiles, then beneficial in chocolates [3].
Tscheuschner	$\tau = \tau_0 + a\gamma + b\gamma^c$	Quattro-parametral form of S-B model [21,24] by Tscheuschner [3,25], based Bauer [24,26].
Balan	$\tau = \tau_0 + \eta\gamma\left[\frac{1 + (q_1 q_2 \gamma^2)}{1 + q_1^2 \gamma^2}\right]$	Proposed by Balan [14], as an extension of Johnson-Segalman [27-29].
Papanastasiou	$\tau = \tau_0(1 - e^{-\omega\gamma}) + \eta\gamma$	Solved S-B and H-B models weakness in continuity at low shear rates [16,19,30].
Dorier-Tichy	$\tau = \left(\frac{2}{\pi}\right)\tau_0 \tan^{-1}\left(\frac{\gamma}{\gamma_0}\right) + \eta\gamma$	Tichy-based S-B model for rheo-electric oils (smart lubricants) [15,31-33].
Windhab	$\tau = \tau_0 + (\tau_1 - \tau_0)\left[1 - e^{\left(-\frac{\gamma}{\gamma^*}\right)}\right] + \eta\gamma$	Better than Casson [34-36].

2.2 Models with shear stress independent of shear rate

In this class of models, the shear strength of the lubricant is assumed to be finite [1,37]. The pioneer of this theory was Smith [1,37–43] who related the formation of an oil film within a contact zone to the oil flow properties and the pattern of shear rate distribution in lubricant film [37,41,44]. According to this theory, lubrication in the contact zone requires plastic deformation whose shear stress is independent of the shear rate [41]. Therefore, a parameter called limiting shear stress or τ_L [1,38–39,42,44-45] (also indicated as τ_{lim} [43] or τ_{LSS} [40,43]) proposed to explain the process of oil film formation and its rheological behavior at high shear rates [41]. Smith's studies showed that the coefficient of tensile friction is always inversely related to the ambient temperature [46]. This relationship is considered important because Smith had assumed in his theory that the tensile friction coefficient determined by shear stress [1], which is independent of the shear rate, and oil film thickness is directly related to the viscosity of the lubricant [1,41]. Such behavior was justified by assuming a completely hydrodynamic film of oil formation at contact point, which has completely non-Newtonian behavior [46] which can be described by the Hersey number [41]. This fluid behavior can be studied in the form of a flow curve [40] shown in Figure 4.

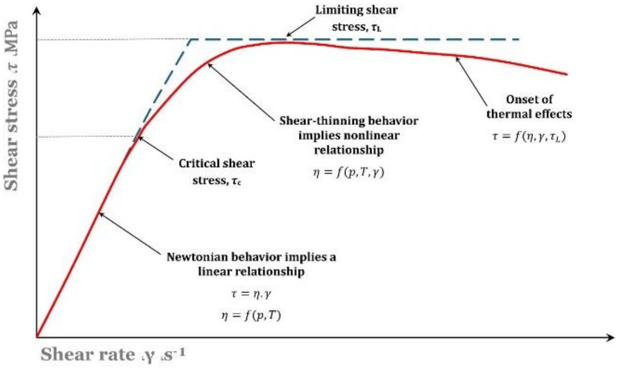

Fig. 4. Typical flow curve for a pressurized lubricant based on shear stress versus shear rate, adapted from [40,43,45].

In the flow curve (Figure 4), as the shear stress increases, the lubricant reaches its critical stress τ_c, which is the amount of shear stress at which the lubricant behavior deviates from Newtonian state and shear-thinning begins (Figure 3), which requires a nonlinear development of shear stress in terms of shear rate [40]. The basis of shear stress theory is a limit that occurs from this point onwards. This is because any ideal Newtonian fluid has the ability to achieve infinite shear stress as the shear rate increases. However, since such behavior is not possible in reality, it is obvious that regardless of shear rate, the shear stress that any fluid is able to transmit must have a finite and specific value [45-46].

The limiting shear stress τ_L is defined as the product of the maximum shear friction coefficient f_{max} multiplied by the normal load F_N divided by Hertzian contact area A (Equation 4 [40]) or the product of the maximum tangential force F_{Tmax} divided by Hertzian contact area A (Equation 5 [42]):

$$\tau_L = \frac{f_{max} F_N}{A} \tag{4}$$

$$\tau_L = \frac{F_{Tmax}}{A} \tag{5}$$

Here, by defining the parameter "average oil pressure in the Hertzian contact zone" or p_m [MPa] [40,42]:

$$p_m = \frac{F_N}{A} \tag{6}$$

In Eq. (6), A is the area of the Hertzian contact zone [mm^2], defined as follows [47]:

$$A = 2b.\, l_{eff} \tag{7}$$

The two parameters b and l_{eff}, in Eq. (7), constitute the effective width and length of the Hertzian region area, respectively [mm], as an Elliptical Contact the details of which are shown in Figure 5 [47]. Recent detailed analyses of rolling-element bearing contacts further confirm the validity of elliptical Hertzian stress distributions and their thermal–mechanical implications under realistic operating conditions [48].

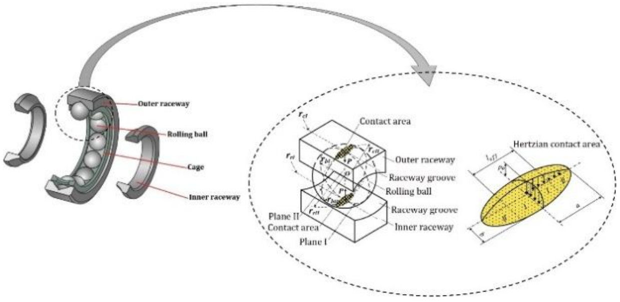

Fig. 5. Hertzian stress exchange area [47-49].

In tribological contacts where principal radii of curvature differ along orthogonal axes, the Hertzian contact area assumes an elliptical shape (as indicated in Fig. 5). The semi-axes of the ellipse, a and b, depend on the applied load, effective elastic modulus, and curvature geometry. The maximum contact pressure is expressed using classical Hertzian relations, which are essential for correlating mechanical stress distribution with local electric field intensification.

Although some references preferred not to provide a formula for calculating the surface area of the Hertzian contact zone A [40,45], some others have assumed the surface area of the Hertzian contact zone to be a circle [42-43] with radius $a_{HERTZ} = \sqrt[3]{\frac{3F_N R}{2E'}}$ [43] and area $A = \pi a_{HERTZ}^2$ [42-43] or a rectangle with length L_x and width L_y with area $A = L_x.L_y$ [43] where the definition of parameters R and E' is available in Figure 6. At the same time, the width of Hertzian contact zone can also be calculated using following equation [39,45]:

$$b = \sqrt{\frac{8wR}{\pi E'}} = \frac{4p_h R}{E'} \tag{8}$$

In Eq. (8), w is the load applied per unit width of the Hertzian contact area, R is the equivalent radius of curvature of the two surfaces R1 and R2, and E' is the equivalent elastic modulus (in GPa [1]), all defined in Figure 6 [39].

For the general case of two bodies in contact with principal radii of curvature that differ in the x- and y-directions, the resulting Hertzian contact region assumes an elliptical shape as shown in Fig. 5. The semi-major (a) and semi-minor (b) axes of the contact ellipse are determined from the applied normal load W, the effective elastic modulus E′, and the combined principal curvature parameters A and B [48-49]:

$$a = \alpha \left(\frac{3W}{2E'}\right)^{1/3}, b = \beta \left(\frac{3W}{2E'}\right)^{1/3} \tag{9}$$

where α and β are geometric coefficients defined by the ratio of principal curvatures and satisfy:

$$\alpha\beta = \left(\frac{1}{A+B}\right)^{1/3} \tag{10}$$

The maximum Hertzian contact pressure for elliptical contact is then expressed as [48-49]:

$$\alpha\beta = \left(\frac{1}{A+B}\right)^{1/3} \tag{11}$$

These relations describe the elliptical pressure distribution that corresponds to the geometry illustrated in Fig. 5 and provide the complete Hertzian framework required for accurate modelling of non-axisymmetric contacts.

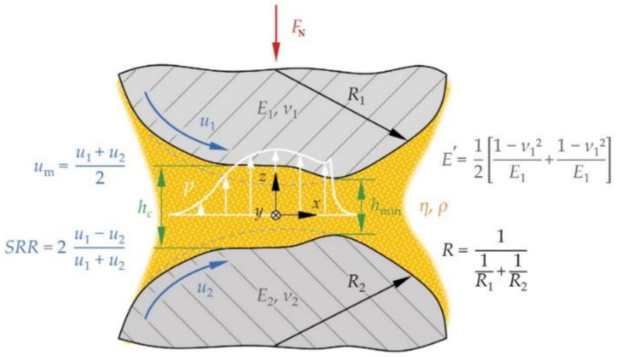

Fig. 6. Hertzian contact and parameters involved [50].

Now, by applying p_m definition from Eq. (6) in Eq. (4) [40,42]:

$$\tau_L = f_{\max} p_m = \frac{F_{T\max}}{A} \tag{12}$$

However, the τ_L can be considered as a result of a lubricant's behavioral failure, can be summarized as the inability of the oil film to support a shear stress that is greater than a certain fraction of the average oil pressure (p_m) in the Hertzian contact zone, as is evident from Eq. (12), this behavioral failure affects oil film shear friction coefficient f_{max} [45]. On the other hand, various references have attempted to relate p_m to p_h [39,42-43,45]:

$$p_m = \begin{cases} \frac{\pi}{4} p_h = 0.785 p_h \\ \frac{2}{3} p_h = 0.667 p_h \end{cases} \tag{13}$$

The method of calculating the p_h will also be different subjective to each reference [39,42-43]:

$$p_h = \begin{cases} \frac{2w}{\pi b} \\ \frac{3}{2}\frac{F_N}{A} = 1.5 p_m \end{cases} \tag{14}$$

The concept of τ_L has been used in different rheological models and has been measured using different experimental methods. The results of these measurements led to a mathematical relationship defining the linear dependence of τ_L on p_m and its local temperature T [°C] [1,38-39,42-43,46]:

$$\tau_L = \tau_{L0} + \varepsilon p_m - \beta T \tag{15}$$

Noteworthy, in some references, linear dependence of τ_L is limited only to oil pressure [1,38-39,43] and the application of the non-negligible contribution of heat to the fluctuation of this concept has been omitted; however, since the thermal contribution of shear stress changes in the study of the behavior of a fluid cannot be ignored [2], it was decided to generalize this equation by resorting to the definitions in other engineering sources [43]. Thus, Eq. (12) has the great advantage that the effectiveness of pressure and temperature on limiting shear stress development is defined separately in it, and therefore, using Eq. (12), contribution of mechanical and thermal effects to the fluctuation of the lubricant's limiting shear stress can be considered separately [43]. The definition of the components of Eq. (12) is presented in Table 2.

Table 2. Parameters in Eq. (12) [1,38-39,42-43].

Parameter	Description	Expression	Range
$\boldsymbol{\tau_{Lo}}$ [MPa]	Initial value of τ_L at zero [1,43]/ambient pressure [38-39]	τ_0 or τ_{L0}	~15 (mineral oils) [1,39] 1~8 [38-39] 2~10 [38] 1~5 [42-43]
$\boldsymbol{\varepsilon}$	The τ_L proportionality coefficient [1,39]	$\partial\tau_L/\partial p_m$ [1,43]	0.05~0.1* [1,42-43] 0.02~0.2† [1] 0.03~0.15 [38-39] 0.02~0.15 [42]
$\boldsymbol{\beta}$ [MPa/°C]	linear graph slope of τ_L versus T [42-43]	$\partial\tau_L/\partial T$	

* For all types of mineral and synthetic oils in the temperature range -27~+40°C and pressure 1.2GPa [1,42]

† This range is recommended for real oils and depends on the type of oil [1]

Jacobson then proceeded to derive a model of oil behavior by combining Newtonian behavior at low pressures with plastic behavior at high pressures and shear stresses to account for different oil film shapes and different pressure distribution patterns in point and linear contact regions [1,38-39]. These studies led to improved estimates of the range of τ_{L0} and ε as the two important parameters constituting Eq. (12) [1,38,42-43]. However, it was Allen who first used Dowson-Higginson equation [51], to calculate the h_{min}.

Allen's studies showed, considering $\tau_L < 0.07 p_h$ (assuming ε=0.07), the exponential growth of dynamic viscosity with respect to oil pressure can be used to estimate h_{min} [1]. However, the author believes using this equation for h_{min} based on the influence of dynamic viscosity on oil pressure in the contact area should be done in line with Jacobson's studies and with regard to the type of contact between two metal surfaces (linear or point). In general, two equations have been proposed to calculate h_{min} based on linear or point contact, which include linear contact [47]:

$$h_{min} = \frac{2.65\alpha^{0.54}(\eta.V)^{0.7}}{\left(\frac{1}{r_1}+\frac{1}{r_2}\right)^{0.43}\left(\frac{Q}{L}\right)^{0.13}}\left[\frac{E}{1-\left(\frac{1}{m}\right)^2}\right]^{-0.03} \tag{16}$$

In Eq. (16), known as Dowson equation used for line contact: α is the coefficient of η change angle against pressure as constant number and defined as logarithmic viscosity-pressure graph slope [m^2/N]. Different relations have been proposed to determine α, among them the following relation was chosen [47]:

$$\alpha = (0.6 + 0.965\log_{10}\eta_0) \times 10^{-8} \tag{17}$$

In Eq. (17), η_0 represents oil dynamic viscosity under atmospheric pressure [Pa.s]. Following to parameters constituting Eq. (16), η represents dynamic viscosity [mPa.s], V is average rollers velocity [m/s] defined as [47]:

$$V = {}^{(V_1 + V_2)}/_{2} \tag{18}$$

The two velocity components V_1 and V_2 in Eq. (18) are, respectively, the rolling element velocity and the velocity at the intersection of the inner and outer contact surfaces [m/s]. Returning to the parameters of Eq. (16), E represents the modulus of elasticity (for steel equal to 2.08×10^5 N/mm^2), r_1 is rolling element radius [mm], r_2 is inner/outer raceway radius [mm], Q is load applied to the rolling element [N], L is the gap length or effective roller length [mm], and 1/m is Poisson's constant (0.3 for steel) [47]. Eq. (16) depicts the point contact between metal surfaces as follows:

$$h_{min} = \frac{3.63\alpha^{0.49}(\eta.V)^{0.68}}{\left(\frac{1}{r_1}+\frac{1}{r_2}\right)^{0.466}Q^{0.073}}\left[\frac{E}{1-\left(\frac{1}{m}\right)^2}\right]^{-0.117}(1 - e^{-0.68k}) \tag{19}$$

In Eq. (19), known as the Hamrock-Dowson equation: *e* represents Euler number equal to 2.7182 and *k* is pressure surface semi-axis ratio or the contact area ellipticity ratio defined as *k*=a/b, where *a* is semi-axis perpendicular to the motion direction and *b* is semi-axis parallel to the motion direction [47].

The h_{min} has strong effect on dynamic viscosity at oil operating temperature η_{0T} [51]; the extent of this effect can be clearly seen in the quasi-harmonic behavior in Figure 7.

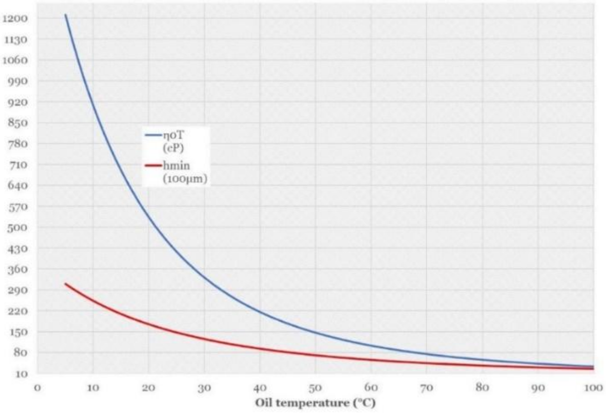

Fig. 7. Effect of η_{0T} changes in the temperature range of 5~100°C on h_{min} for Behran Bordbar PG220 gear oil, adapted from [52].

Accordingly, various models were proposed based on the logic of various mathematical functions in order to best match the laboratory measurement results of shear stress τ, shear rate γ, and dynamic viscosity η, relying on mathematical relationships and observing the principle of independence of shear stress τ from shear rate γ. The description and details of each are presented in Table 3:

Table 3. Rheological models assuming independence of shear stress from shear rate.

Model	Description	Comments
Newton	$\tau = \eta\gamma$	Proposed by Isaac Newton assuming a constant η [1].
Ostwald - de Waele	$\tau = m\gamma^n$ $\begin{cases} n < 1 \longrightarrow \text{Shear}-\text{thinning} \\ n = 1 \longrightarrow \text{Newtonian flow} \\ n > 1 \longrightarrow \text{Shear}-\text{thickening} \end{cases}$	Developed by A.M. de Waele and later by W.F. Ostwald [3,5,53] known as Power-law [1,3,5,7,16,45,53-54].
Steiger-Ory	$\gamma = c_1\tau + c_2\tau^3$	Proposed by K. Steiger and A.M. Ory [3,55-56] as an attempt solving O-dW model failure at low shear rates [57-58].

Model	Description	Comments
Ree-Eyring	$\gamma = p_1 \sinh\left(\frac{\tau}{p_2}\right)$	Originally developed by H. Eyring [3,59] later known as Ree-Eyring model [3,60-61] backed to Prandtl studies [3,59].

Description of mathematical symbols used in this table:

τ: shear stress, [Pa]; η: dynamic viscosity, [Pa.s]; γ: shear rate, [s^{-1}] [3].

m: Power-law coefficient [1] /flow coefficient [3] /consistency coefficient [3,7,36] /consistency index [5,16], [Pa.s] [3,5,7,36]; n: Power-law index [1,3] /flow index [3] /Power-law exponential index [7] /rate index [36] which is a constant and dimensionless number [5]; c_1 and c_2: Steiger-Ory coefficients [3,57] /constant and dimensionless numbers [58,62] /rheological system parameters [56], $[\frac{1}{Pa.s}]$ for c_1 and $[\frac{1}{Pa^3.s}]$ for c_2; p_1: Eyring-Prandtl-Ree coefficient or EPR for short, [1/s]; p_2: scaling factor, [Pa] [3].

Thus, by identifying the relationship between the components affecting the rheological behavior of a lubricant, it is now possible to define the rheological properties of a typical lubricant.

3. RHEOLOGICAL PROPERTIES

Undoubtedly, the lubricant's viscosity constitutes the most important part of its rheological behavior. However, since relying solely on viscosity cannot be a suitable and comprehensive measure for understanding the rheological behavior and the flow behavior of a lubricant at different temperatures and pressures [1], therefore, in addition to viscosity, other parameters that contribute to the rheological behavior of a lubricant will be introduced in this article. Recent comprehensive reviews of experimental data on lubricant density, viscosity, and phase behavior—including refrigerant–lubricant mixtures—highlight the strong interdependence of these properties under varying thermodynamic conditions [63]. In the previous section, the ultimate shear stress τ_L and the shear friction coefficient f_{max} important and unavoidable effect on the quality of oil film formation revealed. On the other hand, in heavy loads, the elastic deformation of the rollers (Figure 8) can be larger than the elastic or viscous deformation of the oil film [1].

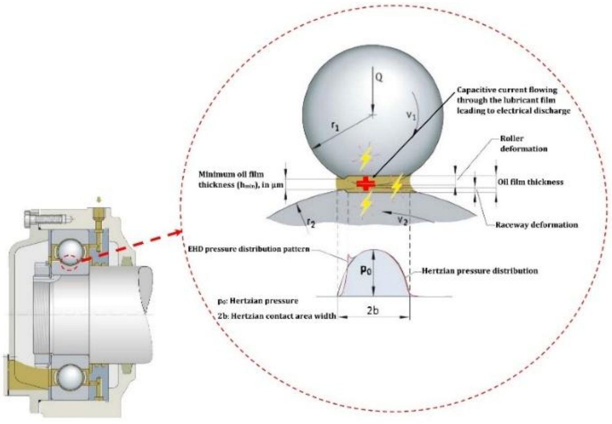

Fig. 8. Roller and ring deformation during oil film formation and electrostatic discharge [49].

Therefore, since a parameter such as τ_{L0} is not easy to measure [38-39], calculating the shear stress τ in order to obtain a correct estimate of viscosity and, consequently, h_{min} will not be an easy process. Accordingly, rheological properties affecting lubrication quality can be divided into the following.

3.1 Viscosity

Viscosity plays a primary role in determining load-carrying capacity, film formation, and shear response in lubricated contacts. Under high pressure and temperature gradients, viscosity affects the evolution of electric field distribution within the lubricant film, influencing charge relaxation and dielectric stability.

Non-Newtonian behavior, including shear thinning and localized viscosity collapse in thin films, alters how charges move and accumulate within the lubricant. These behaviors directly influence dielectric breakdown, resistive heating, and electrostatic discharge phenomena.

Thus, viscosity is not only a mechanical parameter but also a determinant of electro-responsive behavior, linking rheology to electrical performance within the rheo-electric framework. Generally, there are two quantitative methods for expressing viscosity in the engineering literature:

- Absolute or dynamic [2] or shear [3] viscosity, represented by the Greek letter η [2-3], is defined as the intermolecular force that is interpreted as the drag force resisting the applied shear stress or the resistance of the inner layers of the oil film to displacement due to the application of force. Thus, the dynamic viscosity η in an oil is not related to the type of oil but to the flow regime, temperature, and pressure of the oil, the unit of measurement of which is Pa.s [2], although the use of other units, including P (poise) [3], for it is quite possible in the engineering literature. So far, several equations have been proposed to calculate the dynamic viscosity of an oil in terms of temperature, among which Reynolds, Andrade, Slotte, and Barr can be mentioned, the exponential form of the Barr equation having the highest accuracy among others [2,64]:

$$\eta = ae^{\left[\frac{b}{(T-c)}\right]} \tag{20}$$

In Eq. (20), the letters a, b, and c are constant coefficients that are determined according to the behavior of each oil [2].

- Kinematic viscosity, the concept of which was first proposed by Poiseiulle. This concept, which was initially very brief and concise, entered the engineering literature, by definition, is the time it takes for a certain amount of oil (mass flow rate) to travel a certain distance without the intervention of an external force and solely relying on the force of gravity (dependent on the density of the oil). Thus, the kinematic viscosity of the lubricant, which is represented by the Greek letter ν [1-3], in addition to the oil flow regime and the temperature and pressure resulting from it, depends on the type of oil in general (and its density in particular) and can be expressed in the unit of measurement mm^2/s or cSt [2-3]:

$$\nu = \frac{\eta}{\rho} \tag{21}$$

As with dynamic viscosity, various equations have been proposed to estimate kinematic viscosity in terms of oil temperature changes, of which the Walther-Manning equation [8] is considered the best option:

$$\log_{10}\left\{\log_{10}\left[\nu + 0.7 + e^{-(1.47+1.84\nu+0.51\nu^2)}\right]\right\} = A - B\log_{10} T \tag{22}$$

In Eq. (22), A and B are constant numbers determined by using the ASTM diagram [8].

3.2 Density

Like viscosity, density is also a performance property of a lubricant that affects the Newtonian or non-Newtonian rheological behavior of the lubricant in accordance with temperature and pressure [4]. Density is a physical characteristic of a lubricant [1,2,10] can be defined as:

$$\rho = \frac{m}{\mathrm{v}} \tag{23}$$

In Eq. (20); m represents the mass of the lubricant in kg and v represents its volume in m^3 [1,12]. Therefore, the density of a lubricant, represented by the Greek letter ρ, is an indicator of change in mass per unit volume of lubricant in kg/m^3 [1,12,20,42,45,65]. Although the density changes along the oil film height are assumed to be negligible and small (in other words: $\frac{\partial \rho}{\partial z} = 0$ [15,37]), just like dynamic viscosity, its dependence on temperature, pressure, and shear rate [43] governing the oil flow is undeniable [1,5,10,15,39,43,53,66]. The dependence of density on temperature can be expressed through the following relationship [1]:

$$\frac{1}{\mathrm{v}}\frac{\partial \mathrm{v}}{\partial T} = -\frac{1}{\rho}\frac{\partial \rho}{\partial T} \tag{24}$$

Thus, the density of the oil (as a function of temperature) at any temperature point can be calculated [1-2]:

$$\rho_T = \rho_{15}[1 - \alpha_{15}(T - 15)] \tag{25}$$

In Eq. (25); ρ_T represents the density of the oil at any temperature point, ρ_{15} represents the density of the oil at 15°C [2,10], and α_{15} represents the coefficient of volumetric expansion of the oil at 15°C [2]. As can be seen from Eq. (25), since the density of each lubricant is a number unique to that lubricant, then with a change in the temperature of that lubricant, we will witness a change in its density due to the coefficient of thermal expansion α_T. This means that as the temperature of the oil decreases, its mechanical compressibility in order to transform from liquid to solid phase behavior will also decrease [1]. This phenomenon indicates the strong effect of the density of an oil on its rheological behavior.

In comparison, the density of the lubricant is less affected by pressure than viscosity [1-2,5]. However, at high pressures, which exist in the EHL contact zones, and in such conditions the oil film practically exhibits plastic and quasi-solid behavior, where the incompressibility condition is no longer valid and we practically witness a completely compressible material, the effect of pressure on the density of the oil film cannot be ignored [2]. Recent thermophysical modeling studies have demonstrated that lubricant density under combined pressure–temperature loading can be accurately predicted using a minimal set of experimental inputs, enabling reliable extrapolation to EHL-relevant conditions and lubricant–refrigerant mixtures [67]. In this case, by introducing the parameter $\bar{\rho}$ as the dimensionless density of the Dowson-Higginson relation, we have [1,4,39]:

$$\bar{\rho} = \frac{\rho}{\rho_0} = 1 + \frac{0.6E'P}{1+1.7E'P} \tag{26}$$

Where in Eq. (26); ρ_0 is the density of the oil at atmospheric pressure in kg/m^3, E' is the equivalent modulus of elasticity (defined in Figure 6), and P represents the dimensionless pressure $P = \frac{p}{E'}$ [1].

3.3 Viscosity-Pressure coefficient

As noted earlier in Section 3.1, the dynamic viscosity of a lubricant depends not only on temperature but also on pressure; however, no explicit formulation was previously introduced to describe the quantitative relationship between these two scalar variables. In practice, the pressure dependence of lubricant viscosity cannot be meaningfully characterized without defining the slope of the viscosity–pressure relationship. This slope, which reflects the sensitivity of viscosity to pressure variations, is regarded in this study as a fundamental rheological property of lubricants. Accordingly, a detailed treatment of the pressure–viscosity relationship is intentionally deferred to the present section.

Given the importance of calculating oil viscosity at different pressures, several mathematical equations have been proposed to explain the behavior of oil against pressure, the most famous of which is the Barus equation [1,4,8,68] and is suitable for working pressures up to 0.4 GPa [8]:

$$\eta_p = \eta_0 e^{\alpha p} \tag{27}$$

In Eq. (27); η_p is the dynamic viscosity of the oil at pressure p [Pa.s] [8], η_0 is the dynamic viscosity of the oil at atmospheric pressure (equal to 100kPa) [Pa.s] [1,4,8], and α is the slope of the viscosity development graph η_p in terms of p (or in other words: $\alpha = \frac{\partial \ln \eta_p}{\partial p}$) [Pa^{-1}] [1,4,8,68-69]. In fact, α is a constant number that expresses the slope of the logarithmic graph of dynamic viscosity versus pressure, and various relations have been proposed to determine it so far. By definition, the slope of the viscosity-pressure diagram α in an oil represents the relationship between the pressure exerted on the oil film in a conventional Hertzian contact region with the minimum thickness h_{min}, which is a function of the temperature and oil pressure, and the following relationship is one of the best relationships for calculating it in various types of lubricants [8]:

$$\alpha = \alpha(p, T) = \frac{(\ln \eta_p - \ln \eta_0)}{p - p_0} \tag{28}$$

In Eq. (28), p_0 denotes the atmospheric pressure, taken as 100 kPa. This equation indicates that the pressure–viscosity coefficient α follows an exponential dependence on the pressure-dependent viscosity η_p, such that a decrease in temperature is generally associated with a pronounced increase in the value of α. Accurate determination of the pressure–viscosity coefficient α has been shown to depend strongly on both film-thickness modeling accuracy and experimental resolution [70], while numerical studies of industrial gear contacts confirm its decisive role in elastohydrodynamic film formation and wear prediction across different base oils [71]. Recent investigations, however, have demonstrated that the presence of viscosity-index-improving additives can significantly alter the conventional temperature–pressure behavior of α, an effect that is particularly pronounced under elastohydrodynamic lubrication (EHL) conditions. Depending on the concentration of these additives and the molecular weight distribution of the base oil, the rheological response governing oil film formation may deviate substantially from classical expectations. Specifically, the oil film thickness may decrease at low temperatures while increasing at elevated temperatures, implying an anomalous increase of α at higher temperatures when a sufficient concentration of viscosity-index improvers is present.

Despite its widespread use, Eq. (27), commonly referred to as the Barus equation, exhibits limited accuracy at pressures exceed approximately 0.5 GPa. Moreover, even under the piezoviscous assumption of temperature-independent viscosity–pressure behavior, its predictive capability deteriorates further as temperature increases [8]. This limitation arises in part from the definition of α itself and from the extent to which it influences lubricant behavior at the inlet of the Hertzian contact zone [72]. In practice, accurate determination of α at elevated temperatures requires knowledge of the lubricant's piezoviscous response at pressures that are often an order of magnitude greater than the EHL inlet pressure and may approach or exceed the maximum Hertzian contact pressure. Consequently, existing definitions of α remain largely restricted to predicting the rheological behavior of fluids with high Newtonian limits at relatively low temperatures. It is therefore reasonable to conclude that, despite more than five decades of refinement in film thickness estimation methods for EHL contacts, a universally accepted and comprehensive definition of the pressure–viscosity coefficient α capable of fully characterizing piezoviscous behavior in the EHL regime has yet to be established [68].

3.4 Thermal conductivity

The thermal conductivity of a lubricant, denoted here by λ [$W\cdot m^{-1}\cdot K^{-1}$] [1,4,10,42–43,45,64], constitutes a fundamental property governing the rheological–thermal response of lubricated contacts. It plays a decisive role in determining the spatial distribution of heat within a given oil-film geometry [1] and, similar to viscosity, exhibits a strong dependence on both temperature [4,16,64] and pressure [4,64] under flowing conditions [64]. In recent years, advanced experimental methodologies based on thermoelectric principles have been introduced to enhance the accuracy of thermal conductivity measurements in fluids under well-controlled thermal and hydrodynamic environments [73]. Complementary to experimental approaches, data-driven thermophysical models have been proposed to predict lubricant thermal conductivity across wide temperature and pressure ranges using limited calibration datasets, significantly reducing experimental demand while maintaining accuracy [67].

Notably, the sensitivity of thermal conductivity to pressure is substantially greater than its sensitivity to temperature [4,64]. Experimental evidence indicates that an increase in oil pressure to approximately 1 GPa can result in a twofold increase in thermal conductivity [64]. Consequently, at relatively low pressures, thermal conductivity decreases with increasing temperature, whereas under high-pressure conditions this trend is reversed, giving rise to a distinct turning point in the temperature dependence of thermal conductivity [4]. The thermal conductivity of lubricating oils may be mathematically described using Fourier's law of heat conduction [4,16,18,45,53,64]:

$$\lambda \frac{\partial^2 T}{\partial z^2} = -\tau\gamma \tag{29}$$

In the topic of predicting and estimating the rheological behavior of a lubricant and the formation of an oil film (often expressed in the engineering literature as h_{min}) in the EHL contact zones, assuming isothermality, it is only necessary to consider the dependence of viscosity and density on pressure in the problem and perform the necessary calculations to determine h_{min}. However, in non-isothermal problems, since the determination of the temperature distribution pattern also enters the problem, in addition to the classical dependence of viscosity and density on temperature and pressure, solving the problem in the simplest case requires considering the influence of the thermal conductivity of the oil film on pressure [4]. This topic is most widely used in predicting the rheological behavior of automatic transmission and heat transfer oils (especially in electric vehicles) [15], hydraulic, compressor, metal forming oils, and some greases [10]. Because at the moment of entering the Hertzian contact zone, the oil flow has endured very high shear rates and it is in such a state that the contribution of convective heat transfer pales in comparison to conductive heat transfer. This is where the role of the thermal conductivity λ of the oil and the turning point of its behavior change against temperature under the influence of low and high pressures prevailing before and within the EHL contact zone becomes of undisputed importance [18].

4. RHEO-ELECTRICAL PROPERTIES

Electrical conductivity, electrical resistivity, dielectric permittivity, and charge-relaxation characteristics collectively govern the response of lubricants when subjected to external electric fields. Recent experimental studies have demonstrated a strong dependence of lubricant permittivity on both pressure and temperature in hydrodynamic bearing applications, confirming the sensitivity of dielectric behavior under operating conditions [11]. These parameters directly affect molecular polarization and alignment within the lubricant, field-induced modifications of apparent viscosity, and the material's susceptibility to dielectric breakdown and electrostatic discharge phenomena.

Although the coupling between electrical and rheological properties of lubricants has been previously addressed in the engineering literature—primarily to elucidate electrically induced surface damage mechanisms such as current burning, fluting, frosting, and micro-cratering, which are commonly classified as forms of electrical erosion [47]—these studies have typically appeared under broader conceptual frameworks, including electrorheology [74–75], electro-rheology [76], or triboelectricity [77–78]. In contrast, the present author has formally introduced the terms rheoelectricity and rheo-electrical properties in prior works [47,64], together with dedicated mathematical formulations that explicitly relate the rheological behavior of lubricants to their electrical characteristics.

4.1 Mason Number and Field-Induced Response

Rheo-electrical properties have played a significant role, especially in investigating phenomena such as fluting and micro-cratering as a subset of electrical erosion in various components of electromechanical machinery and electric vehicles, and understanding how each interacts with internal and external factors affecting the failure of this type of machinery can lead to a clear picture of the failure mechanism and provide a solution to avoid the recurrence of failure in such equipment. Of course, to better present such a picture, aggregation indices such as the Mason number [15] have been defined, which expresses the ratio of hydrodynamic forces to electrostatic forces [15,79-80] of the particles forming the oil flow:

$$Ma = \frac{F^H}{F^P} \qquad (30)$$

In Eq. (30), F^H represents the shear forces between particles forming the oil flow, leading to the crystallization of the hydrodynamic behavior affected by the rheology of the oil, which is defined as follows [15,80]:

$$F^H = 6\pi r^2 \eta\gamma \qquad (31)$$

In Eq. (31), the term r represents the particle radius [13] in μm. On the other hand, F^P in Eq. (30) represents the electrostatic forces between the particles forming the oil flow [15], which is defined as [15,80]:

$$F^P = 12\pi\varepsilon_{oil}(r.\beta.E)^2 \qquad (32)$$

In Eq. (32), E represents the electric field strength [15] in V/m [47], and β is the relative polarizability [80], which can be defined as follows [15]:

$$\beta = \frac{(\varepsilon_p - \varepsilon_{oil})}{(\varepsilon_p + 2\varepsilon_{oil})} \qquad (33)$$

The parameter ε_p in Eq. (33) is the dielectric constant of charged particles suspended through the oil flow [15,80]. Thus, according to Eq. (31) to (33) and by applying the definition $\tau=\eta\gamma$, the Mason number defined in Eq. (30) can be rewritten as follows [15,80]:

$$Ma = \frac{F^H}{F^P} = \frac{\tau}{2\varepsilon_{oil}(\beta.E)^2} \qquad (34)$$

A low Mason number corresponds to a low shear-rate regime, in which electrostatic forces dominate the rheological response of the lubricant. Under such conditions, the lubricant exhibits an increased tendency toward elevated yield stress and quasi-solid behavior when subjected to an external electric field. Conversely, a high Mason number—approaching asymptotically large values—indicates that hydrodynamic shear forces prevail over electrostatic interactions. In this regime, the apparent dynamic viscosity increases in a nearly linear manner characteristic of Newtonian fluids [15], resulting in quasi-fluid behavior of the lubricant film and a pronounced tendency to flow under minimal applied yield stress.

One of the most significant practical implications of lubricant rheoelectricity lies in the diagnosis and prevention of electromechanical equipment failures, particularly those associated with electrostatic discharge–induced damage. Rheo-electric analysis further enables the prediction of lubricant aging mechanisms driven by thermally induced stresses arising from asymmetric ionization within localized volumes of the lubricant film. Equally important is the reciprocal influence of the lubricant's rheo-electrical properties on the resulting electromagnetic interactions, which can substantially affect oil-film behavior under the simultaneous presence of electric and magnetic fields. This coupled behavior can be quantitatively assessed through the combined analysis of dimensionless parameters such as the Mason and Bingham numbers.

The Mason number (Mn), defined as a dimensionless ratio of viscous to electrostatic forces acting within a lubricant exposed to an electric field, therefore serves as a valuable indicator for predicting rheo-electric transitions and assessing stability in electrically stressed lubrication regimes.

Based on these considerations, the principal rheo-electrical properties of a representative lubricant are summarized in Table 4.

Table 4. Rheo-electric properties of a typical lubricant.

Parameter	Expression	Description
Electrical Conductivity [pS/m]	$\kappa = f(p,T) = \frac{\lambda}{L}\left[\frac{b}{\ln\left(\frac{\eta}{a}\right)} + c\right]$	Temperature effect on lubricant's electrical conductivity is known [64,81], pressure effect is negligible in synthetics [64].
Electrical Resistivity [GΩ/m]	$\rho_s = f(p,T) = \frac{1}{\kappa}$	Increasing temperature causes a sharp decrease in lubricant's resistivity.
Dielectric Dissipation Factor	δ	Measured as per IEC 60247 [64], defined as an index in determining lubricant dielectric loss.
Dielectric Constant	$\varepsilon_{\mathrm{oil}}$	$\varepsilon_{\mathrm{oil}}$ is a lubricant ability as dielectric conductor to become polarized under given electric field leading oil film acts as capacitor [47,82].
Capacitance [pF]	$C_{oil} = \varepsilon_{oil}\left(\frac{A_{HERTZ}}{h_{min}}\right)$	Rheo-electric property inversely proportional to the h_{min}; increasing h_{min} will reduce the oil film capacitance and, consequently, increase lubricant susceptibility to dielectric breakdown and electrical discharges [47].
Dielectric Break-down [V]	$U_b = f(p,T) = E_c . h_{min} = n(\alpha^{0.49} . \eta^{0.68})$	U_{b}, in fact, is the potential difference between two points located on either side of the h_{min} (as anode-cathode). Dielectric breakdown occurs when the electric field intensity formed at cathode exceeds E_{c} [47] and ionization located on anode is facilitated [47].

Description of mathematical symbols used in this table:
λ: thermal conductivity of oil, [W/m°K]; L: Lorenz constant approximately equal to 2.445×10-8, [V^2/K^2]; η: dynamic viscosity, [cP]; a, b, & c: constants of the exponential form of the Barr equation [47].
A_{HERTZ}: Hertzian contact surface area, [mm^2]; h_{min}: minimum oil film thickness, [μm] [47]; E_{c}: critical electric field intensity, [V/m];
n: constant; α: slope of the logarithmic viscosity-pressure plot, as a constant number [47].

5. CONCLUSION

Rheoelectric interactions influence a wide range of degradation processes, including localized dielectric breakdown, electrostatic discharge machining (EDM-like effects), frosting, pitting, and surface material transfer. The balance between shear, viscosity, electric field strength, and dielectric behavior determines the likelihood of failure.

This review establishes rheoelectricity as a critical framework for understanding the coupled electrical and mechanical behavior of lubricants in modern electromechanical systems. By consolidating findings across rheology, tribology, and electro-physics, the article provides a structured basis for interpreting field-dependent lubrication behavior and associated failure modes. Additionally, the review highlights the reciprocal effect of rheo-electric behavior on electrostatic discharge (ESD), emphasizing how field-dependent viscosity, dielectric strength, and charge relaxation mechanisms directly modulate the onset, intensity, and propagation of ESD within lubricated contacts.

REFERENCES

[1] B. O. Jacobson, *Rheology and Elastohydrodynamic Lubrication*. New York, NY, USA: Elsevier, 1991.

[2] A. R. Aminian, "Viscosity—Part I (ویسکوزیته-بخش اول)," *Maintenance in Oil, Gas, & Petrochemical Industries*, vol. 5, no. 24, pp. 36–56, Jul. 2020.

[3] T. G. Mezger, *The Rheology Handbook for Users of Rotational and Oscillatory Rheometers*, 5th ed. Hanover, Germany: Vincentz Network, 2020.

[4] Q. J. Wang and Y. W. Chung, *Encyclopedia of Tribology*. New York, NY, USA: Springer, 2013.

[5] F. A. Morrison, *Understanding Rheology*. New York, NY, USA: Oxford Univ. Press, 2001.

[6] Y. Sosa, "Improving fuel efficiency by selecting the right oil," *Tribology & Lubrication Technology*, pp. 32–37, Jan. 2023.

[7] J. De Vicente, *Rheology*. Rijeka, Croatia: InTech, 2012.

[8] A. R. Aminian, "Viscosity—Part II (ویسکوزیته-بخش دوم)," *Maintenance in Oil, Gas, & Petrochemical Industries*, vol. 6, no. 25, pp. 57–69, Jan. 2021.

[9] C. H. Kuo, *Tribology—Lubricants and Lubrication*. London, U.K.: InTech, 2011.

[10] T. Mang and W. Dresel, *Lubricants and Lubrication*, 2nd ed. Weinheim, Germany: Wiley-VCH, 2007.

[11] B. Prase, F. Koetz, E. Kirchner, and A. Hasse, "Pressure and temperature dependence of the permittivity of mineral and PAG oils for hydrodynamic journal bearing applications," *Lubricants*, vol. 13, no. 12, Art. no. 539, 2025, doi: 10.3390/lubricants13120539.

[12] N. G. Hentz and J. T. Bradshaw, "Guide to liquid volume measurements: A review of methods and technologies," *SLAS Technol.*, vol. 36, Art. no. 100382, 2026, doi: 10.1016/j.slast.2025.100382.

[13] A. R. Aminian, "Viscosity—Part III (ویسکوزیته-بخش سوم)," *Maintenance in Oil, Gas, & Petrochemical Industries*, vol. 6, no. 26, pp. 35–43, Mar. 2021.

[14] V. Radulescu and I. Radulescu, "Rheological models for lithium and calcium greases," *Mechanika*, vol. 59, no. 3, pp. 67–70, 2006.

[15] X. Wang, Q. J. Wang, N. Ren, and R. England, "Lubrication subjected to effects of electric and magnetic fields: Recent research progress and a generalized MEMT-field Reynolds equation," *Frontiers in Mechanical Engineering*, vol. 9, Art. no. 1334814, 2024, doi: 10.3389/fmech.2023.1334814.

[16] W. T. Wu and M. Massoudi, *Recent Advances in Mechanics of Non-Newtonian Fluids*. Basel, Switzerland: MDPI, 2020.

[17] J. Peng, Y. Guangxin, W. Jianping, W. Xiaocui, and W. Xiaolei, "Thermorheological properties of magnetorheological grease and its thermomagnetic-coupling mechanism," *J. Intell. Mater. Syst. Struct.*, vol. 33, no. 3, pp. 432–444, 2021, doi: 10.1177/1045389X211018850.

[18] J. J. Kauzlarich and J. A. Greenwood, "Elastohydrodynamic lubrication with Herschel–Bulkley model greases," *ASLE Trans.*, vol. 15, no. 4, pp. 269–277, 1972, doi: 10.1080/05698197208981427.

[19] D. Bauer, L. Talon, Y. Peysson, H. B. Ly, G. Batôt, T. Chevalier, and M. Fleury, "Experimental and numerical determination of Darcy's law for yield stress fluids in porous media," *Phys. Rev. Fluids*, vol. 4, no. 6, Art. no. 063301, 2019, doi: 10.1103/PhysRevFluids.4.063301.

[20] K. E. Ryl'tseva and G. R. Shrager, "Characteristics of viscoplastic fluid flow at various heat transfer regimes on the walls of a sudden contraction channel," *J. Eng. Phys. Thermophys.*, vol. 96, no. 3, 2023, doi: 10.1007/s10891-023-02726-9.

[21] R. Kozdrach, "The influence of base oil type on the rheological properties of ecological lubricating greases," *Nafta-Gaz*, vol. 77, no. 2, pp. 127–135, 2021, doi: 10.18668/NG.2021.02.07.

[22] J. Pan, Y. Cheng, A. Vacca, and J. Yang, "Effect of temperature on grease flow properties in pipes," *Tribology & Lubrication Technology*, pp. 40–54, May 2018.

[23] W. H. Herschel and R. Bulkley, "Konsistenzmessung von Gummi-Benzollösungen," *Kolloid-Zeitschrift*, vol. 39, pp. 291–300, 1926, doi: 10.1007/BF01432034.

[24] L. A. Ferreira, P. Vergne, and D. Berthe, "A contribution to the study of shear rheology of grease," in *Proc. 14th Leeds–Lyon Symp. Tribology*, Lyon, France, Sep. 8–11, 1987.

[25] A. Diab, "Experimental and theoretical investigations on the viscosity of heterogeneous asphalt binders," *J. Elastomers Plast.*, vol. 50, no. 4, 2017, doi: 10.1177/0095244317729555.

[26] R. D. Bauer, "Rheological approaches of arteries," *Biorheology*, vol. 23, no. 1, suppl., pp. 159–167, 1984, doi: 10.3233/BIR-1984-23S129.

[27] D. Broboana and C. Balan, "Investigations on the rheology of water-in-crude oil emulsions," *Sci. Bull. Univ. Politeh. Bucharest, Ser. B: Chem. Mater. Sci.*, vol. 69, no. 3, pp. 35–50, 2007.

[28] C. Balan and R. Fosdick, "A rheological model for materials which support coexistent shear rates," *Int. J. Non-Linear Mech.*, vol. 35, no. 6, pp. 1023–1043, 2000, doi: 10.1016/S0020-7462(99)00077-3.

[29] M. W. Johnson and D. Segalman, "A model for viscoelastic fluid behavior which allows non-affine deformation," *J. Non-Newtonian Fluid Mech.*, vol. 2, no. 3, pp. 255–270, 1977, doi: 10.1016/0377-0257(77)80003-7.

[30] T. C. Papanastasiou, "Flows of materials with yield," *J. Rheol.*, vol. 31, no. 5, pp. 385–404, 1987, doi: 10.1122/1.549926.

[31] J. A. Tichy, "Hydrodynamic lubrication theory for the Bingham plastic flow model," *J. Rheol.*, vol. 35, no. 4, pp. 477–496, 1991, doi: 10.1122/1.550231.

[32] C. Dorier and J. Tichy, “Behavior of a Bingham-like viscous fluid in lubrication flows,” *J. Non-Newtonian Fluid Mech.*, vol. 45, no. 3, pp. 291–310, 1992, doi: 10.1016/0377-0257(92)80065-6.

[33] S. Jang and J. A. Tichy, “Internal damper characteristics of rotor system with submerged ER fluid journal bearings,” *Int. J. Rotating Mach.*, vol. 3, no. 1, pp. 61–71, 1997.

[34] C. Barbosa, F. Diogo, and M. Rui Alves, “Fitting mathematical models to describe the rheological behaviour of chocolate pastes,” in *Proc. Int. Conf. Numerical Analysis and Applied Mathematics*, Rhodes, Greece, Sep. 23–29, 2015.

[35] Y. Wang, W. Yang, Q. Wang, K. Liu, C. Wang, and Q. Chang, “The rheological performance of aqueous ceramic ink described based on the modified Wndhab model,” *Mater. Res. Express*, vol. 7, no. 7, 2020, doi: 10.1088/2053-1591/aba507.

[36] F. Azeddine, P. A. Sergio, L. Angélique, L. El Khadir, I. Ali, and B. El Houssayne, “Rheological behavior and characterization of drinking water treatment sludge from Morocco,” *Clean Technol.*, vol. 5, no. 1, pp. 259–273, 2023, doi: 10.3390/cleantechnol5010015.

[37] P. Sperka, I. Krupka, and M. Hartl, “Lubricant flow in thin-film elastohydrodynamic contact under extreme conditions,” *Friction*, vol. 4, no. 4, pp. 380–390, 2016, doi: 10.1007/s40544-016-0134-6.

[38] J. Ståhl and B. O. Jacobson, “A non-Newtonian model based on limiting shear stress and slip planes—Parametric studies,” *Tribol. Int.*, vol. 36, no. 11, pp. 801–806, 2003, doi: 10.1016/S0301-679X(03)00096-3.

[39] J. Ståhl and B. O. Jacobson, “A lubricant model considering wall-slip in EHL line contacts,” *J. Tribol.*, vol. 125, no. 3, pp. 523–532, 2003, doi: 10.1115/1.1537750.

[40] Z. Ma, Y. Zhao, Y. Han, W. Lou, S. Li, X. Wang, F. Guo, and H. Liu, “Approach to determine the limiting shear stress of lubricants at high pressures based on traction mapping,” *Lubricants*, vol. 12, no. 4, 2024, doi: 10.3390/lubricants12040128.

[41] F. W. Smith, “Lubricant behaviour in concentrated contact systems—the castor oil–steel system,” *Wear*, vol. 2, no. 4, pp. 250–264, 1959.

[42] S. N. Ndiaye, *Ultimate Behavior of Confined Fluids Under Very High Pressure and Shear Stress*, Ph.D. dissertation, Mécanique, Energétique, Génie civil, Acoustique (MEGA), Génie Mécanique, Université de Lyon, Lyon, France, 2017.

[43] R. Xu, *A Quantitative Approach to EHD Friction Prediction Based on Rheometry and Molecular Dynamics Simulations*, Ph.D. dissertation, Mécanique, Energétique, Génie civil, Acoustique (MEGA), Génie Mécanique, Université de Lyon, Lyon, France, 2023.

[44] F. W. Smith, “Lubricant behavior in concentrated contact—Some rheological problems,” *Tribol. Trans.*, vol. 3, no. 1, pp. 18–25, 1960, doi: 10.1080/05698196008972381.

[45] S. Bair, *High-Pressure Rheology for Quantitative Elastohydrodynamics*. Amsterdam, The Netherlands: Elsevier, 2007.

[46] F. W. Smith, “The effect of temperature in concentrated contact lubrication,” *Tribol. Trans.*, vol. 5, no. 1, pp. 142–148, 1962, doi: 10.1080/05698196208972461.

[47] A. R. Aminian, “Rheoelectricity of turbine lubricants and its effect on the failure process of this category of rotating equipment (رئوالکتریسیته روانکارهای توربینی و تاثیر آن بر روند خرابی این دسته از تجهیزات دوار),” in *Proc. 9th Int. Conf. Technology Development in Oil, Gas, Refining and Petrochemicals (OilBNCF’9)*, Tehran, Iran, Sep. 22, 2025.

[48] F. De Cadier de Veauce, *Étude des sources de pertes et des transferts thermiques au sein de paliers à éléments roulants*, Ph.D. dissertation, INSA de Lyon, Lyon, France, 2024, NNT: 2024ISAL0045.

[49] K. L. Johnson, *Contact Mechanics*. Cambridge, U.K.: Cambridge Univ. Press, 1985.

[50] M. Marian, M. Bartz, S. Wartzack, and A. Rosenkranz, “Non-dimensional groups, film thickness equations and correction factors for elastohydrodynamic lubrication: A review,” *Lubricants*, vol. 8, no. 10, 2020, doi: 10.3390/lubricants8100095.

[51] A. R. Aminian, “Water detection in PAG gear oil: Case study—Part II (تشخیص آب در روغن پی‌ای‌جی گیربکس: مطالعه موردی—بخش دوم),” *Maintenance in Oil, Gas, & Petrochemical Industries*, vol. 7, no. 34, pp. 66–70, Jul. 2022.

[52] A. R. Aminian, “Water detection in PAG gear oil: Case study—Part IV (تشخیص آب در روغن پی‌ای‌جی گیربکس: مطالعه موردی—بخش چهارم),” *Maintenance in Oil, Gas, & Petrochemical Industries*, vol. 7, no. 36, pp. 66–77, Nov. 2022.

[53] V. M. Shapovalov, “On the applicability of the Ostwald–de Waele model in solving applied problems,” *J. Eng. Phys. Thermophys.*, vol. 90, no. 5, pp. 1213–1218, 2017, doi: 10.1007/s10891-017-1676-9.

[54] L. Qiao, A. Nadine, M. Pierre, B. Yves, G. Manuel, and D. Rémi, "A local power law versus a well-identified viscosity curve over a large shear rate range in thermorheology of polymers," in *Proc. 26th Int. ESAFORM Conf. Material Forming*, Kraków, Poland, Apr. 19–21, 2023.

[55] M. Ślęzak, "Mathematical models for circulating the value of dynamic viscosity of a liquid," *Arch. Metall. Mater.*, vol. 60, no. 2, pp. 581–589, 2015, doi: 10.1515/amm-2015-0177.

[56] P. Haũgen, J. O. Rnikis, and M. A. Tung, "Rheological models for dispersions of polyoxyethylene (4) lauryl ether in hydroxyethyl cellulose," *J. Texture Stud.*, vol. 3, no. 2, pp. 233–245, 1972, doi: 10.1111/j.1745-4603.1972.tb00627.x.

[57] AMETEK Brookfield Inc., *RSO Rheometer Operating Instructions*, M19-230-REV.B, p. 52, 2020.

[58] J. M. Tiffany, "The viscosity of human tears," *Int. Ophthalmol.*, vol. 15, no. 6, pp. 371–376, 1991, doi: 10.1007/BF00137947.

[59] H. Eyring, "Viscosity, plasticity, and diffusion as examples of absolute reaction rates," *J. Chem. Phys.*, vol. 4, no. 4, pp. 283–291, 1936, doi: 10.1063/1.1749836.

[60] T. Ree and H. Eyring, "Theory of non-Newtonian flow. I. Solid plastic system," *J. Appl. Phys.*, vol. 26, no. 7, pp. 793–800, 1955, doi: 10.1063/1.1722098.

[61] S. Bair, "Actual Eyring models for thixotropy and shear-thinning: Experimental validation and application to EHD," *J. Tribol.*, vol. 126, no. 4, pp. 728–732, 2004, doi: 10.1115/1.1792693.

[62] P. Travnick, E. Krcalova, and T. Vitez, "Rheopectic behavior of rendered fat," *Pol. J. Environ. Stud.*, vol. 22, no. 5, pp. 1499–1504, 2013.

[63] C. Cikmaz, X. Yang, and M. Richter, "Review of experimental data on density, viscosity, and phase behavior of lubricant oils and their mixtures with refrigerants," *Int. J. Refrig.*, 2025, doi: 10.1016/j.ijrefrig.2025.12.014.

[64] A. R. Aminian, "A comparison of the rheo-electric behavior of two mineral and synthetic ester oils to investigate the scope of each in the lubrication of electric vehicles (مقایسه‌ای از رفتار رئو-الکتریک دو روغن مینرال و سینتتیک استر به‌منظور بررسی دامنه کاربرد هریک در روانکاری خودروهای الکتریکی)," in *Proc. 3rd Nat. Conf. Industrial Technologies in Mechanical Engineering (ITME2025)*, Arak, Iran, May 28, 2025.

[65] P. Kumar, M. M. Khonsari, and S. Bair, "Full EHL simulations using the actual Ree–Eyring model for shear-thinning lubricants," *J. Tribol.*, vol. 131, no. 1, pp. 118021–118026, 2009, doi: 10.1115/1.3002328.

[66] B. McCoy, "Modeling tools for gear design and failure prevention," *Tribology & Lubrication Technology*, pp. 42–47, Dec. 2021.

[67] X. Yang, C. Hanzelmann, S. Feja, J. P. M. Trusler, and M. Richter, "Thermophysical property modeling of lubricant oils and their mixtures with refrigerants using a minimal set of experimental data," *Ind. Eng. Chem. Res.*, vol. 62, pp. 18736–18749, 2023, doi: 10.1021/acs.iecr.3c02474.

[68] S. Bair, "The unresolved definition of the pressure–viscosity coefficient," *Sci. Rep.*, vol. 12, Art. no. 3422, 2022, doi: 10.1038/s41598-022-07470-3.

[69] S. Bair, "A new high-pressure viscometer for oil/refrigerant solutions and preliminary results," *Tribology & Lubrication Technology*, pp. 60–70, Oct. 2017.

[70] H. van Leeuwen, "The determination of the pressure–viscosity coefficient of a lubricant through an accurate film thickness formula and accurate film thickness measurements," *Proc. Inst. Mech. Eng., Part J: J. Eng. Tribol.*, vol. 223, no. 8, pp. 1143–1163, 2009, doi: 10.1243/13506501JET504.

[71] D. Beyralvand, H. Ghazizade-Ahsaee, F. Banazadeh, and R. Moghaddas, "Numerical analysis of the effect of different parameters on lubrication conditions and the possibility of wear in spur and helical gears in three groups of common base oils in the industry," *Karafan J. Tech. Vocational Univ.*, vol. 21, no. 1, pp. 535–552, Spring 2024, doi: 10.48301/KSSA.2023.394313.2529.

[72] S. Bair, "A traction (friction) curve is not a flow curve," *Lubricants*, vol. 10, no. 9, 2022, doi: 10.3390/lubricants10090221.

[73] A. Moinian, N. Rahbar, A. Abedini Esfahlani, H. Kargarsharifabad, and M. Rafiei, "A novel thermoelectric-based method for measuring the thermal conductivity of fluids: An experimental and thermodynamic modeling approach," *Int. Commun. Heat Mass Transf.*, vol. 172, Art. no. 110161, 2026, doi: 10.1016/j.icheatmasstransfer.2025.110161.

[74] R. Fowler, "20 minutes with Vasu Bala," *Tribology & Lubrication Technology*, pp. 24–30, Apr. 2020.

[75] P. Lee, C. Sanchez, M. Moneer, and A. Velasquez, "Electrification of a mini traction machine and initial test results," *Lubricants*, vol. 12, no. 10, 2024, doi: 10.3390/lubricants12100337.

[76] P. Gupta, P. Dhar, and D. Samanta, "Viscoelasticity–contrast driven electrohydrodynamic behaviour of a droplet-suspended-in-a-confined-liquid configuration," *J. Non-Newtonian Fluid Mech.*, vol. 338, 2025, doi: 10.1016/j.jnnfm.2025.105406.

[77] R. Shah, M. Das, M. H. Kabir, H. Liang, L. Salvi, and T. L. Bunting, “Additive and base oil trends in electric vehicle applications,” *J. Tribol.*, vol. 147, no. 5, pp. 511061–511068, 2024, doi: 10.1115/1.4066650.

[78] N. Gnanaseelan, D. P. Pabba, D. E. Acuña-Ureta, G. Fischerauer, S. Tremmel, and M. Marian, “Two-dimensional layered materials for triboelectric nanogenerators,” *Prog. Mater. Sci.*, vol. 158, Art. no. 101622, 2026, doi: 10.1016/j.pmatsci.2025.101622.

[79] S. G. Sherman, A. C. Becnel, and N. M. Wereley, “Relating Mason number to Bingham number in magnetorheological fluids,” *J. Magn. Magn. Mater.*, vol. 380, pp. 98–104, 2015, doi: 10.1016/j.jmmm.2014.11.010.

[80] D. J. Klingenberg, “Mason numbers for magnetorheology,” *J. Rheol.*, vol. 51, no. 5, pp. 883–893, 2007, doi: 10.1122/1.2764089.

[81] A. R. Aminian, “Oil’s electrical conductivity and electrostatic discharge: A case study—Part I (رسانایی الکتریکی روغن و تخلیه الکترواستاتیک: مطالعه موردی—بخش اول),” *Maintenance in Oil, Gas, & Petrochemical Industries*, vol. 9, no. 44, pp. 26–37, Mar. 2024.

[82] N. Dittes, A. Pettersson, P. Marklund, D. Lang, and P. M. Lugt, “Dielectric thermoscopy characterization of water contaminated grease,” *Tribology & Lubrication Technology*, pp. 60–73, Mar. 2018.